This is an *Accepted Manuscript*, which has been through the Royal Society of Chemistry peer review process and has been accepted for publication.

Accepted Manuscripts are published online shortly after acceptance, before technical editing, formatting and proof reading. Using this free service, authors can make their results available to the community, in citable form, before we publish the edited article. We will replace this *Accepted Manuscript* with the edited and formatted *Advance Article* as soon as it is available.

You can find more information about *Accepted Manuscripts* in the **Information for Authors**.

Please note that technical editing may introduce minor changes to the text and/or graphics, which may alter content. The journal's standard **Terms & Conditions** and the **Ethical guidelines** still apply. In no event shall the Royal Society of Chemistry be held responsible for any errors or omissions in this *Accepted Manuscript* or any consequences arising from the use of any information it contains.

Journal Name

ARTICLE

Trinuclear {Co^{2+}-M^{3+}- Co^{2+}} Complexes Catalyze Reduction of Nitro Compounds

Sumit Srivastava,[a] Manvender S Dagur,[a] Afsar Ali,[a] and Rajeev Gupta*[a]

This work presents synthesis and characterization of trinuclear {Co^{2+}-Co^{3+}-Co^{2+}} and {Co^{2+}-Fe^{3+}-Co^{2+}} complexes with accessible peripheral Co(II) ions. Both trinuclear complexes function as the efficient reusable heterogeneous catalysts for the selective reduction of assorted nitro compounds to the corresponding amines. The mechanistic investigations suggest the involvement of Co(II)-Co(I) cycle in the catalysis.
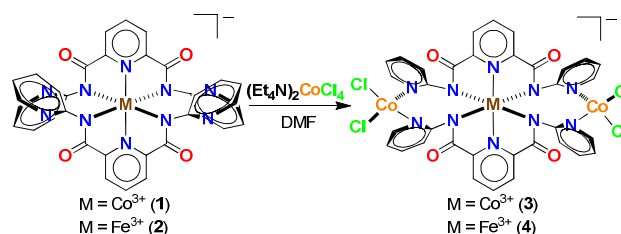
Introduction

Reduction of nitro to the corresponding amine is a fundamental transformation in chemistry as assorted amines constitute an important class of compounds encompassing all aspects of chemical products.[1] In general, reduction of a nitro compound is a straightforward method using an appropriate reducing agent.[2] Such a conversion has been achieved using H$_2$,[3] silanes,[4] boranes,[5] ammonium salts,[6] formic acid,[7] hydrazine,[8] and boron-hydrides;[9] typically in presence of a metal catalyst.[1,2] Such conventional methods generally require stoichiometric or excess amount of metal catalyst as well as reducing agent while H$_2$ often demands high-pressure conditions.[3] Further, several such methods often produce undesirable by-products and suffer due to the lack of selectivity.[10] Furthermore, selectivity in the presence of multiple functional groups still remains a major challenge.[10] As a result, carefully screened and selected precious metal catalysts (such as Pd, Pt, Au, and Ru) are usually required.[11] In recent time, nanoparticles based catalysts have been quite successful as they also control the product selectivity.[12] In particular, nanoparticles based on non-precious metal-oxides, such as Co$_3$O$_4$[13] and Fe$_3$O$_4$[14], have been found exceptionally effective. Although such nanoparticles offer high surface area and therefore high activity they suffer from stability, moisture-sensitivity, special reaction conditions, and lack of reusability. In this context, low-cost earth-abundant metal based heterogeneous and reusable catalysts are highly desirable. Herein, we report trinuclear {Co^{2+}–Co^{3+}–Co^{2+}} (3) and {Co^{2+}–

Fe^{3+}–Co^{2+}} (4) complexes with exposed and catalytically active Co(II) sites and their application as the efficient heterogeneous and reusable catalysts for the hydrazine-based chemo-selective reduction of assorted nitro substrates. We also shed light on the mechanistic aspects of the nitro reduction reactions that suggest the involvement of Co(II)-Co(I) cycle in the catalysis.

Results and Discussion

Synthesis and Characterization of Trinuclear complexes

The metalloligands[15] 1 and 2 on reaction with two equiv. of (Et$_4$N)$_2$CoCl$_4$ produced the trinuclear complexes, {Co^{2+}–Co^{3+}–Co^{2+}} (3) and {Co^{2+}–Fe^{3+}–Co^{2+}} (4) (Scheme 1). Both 3 and 4 are deep green in color and exhibit prominent electronic transitions at 608 and 675 nm in DMF (Fig. S1, ESI). Such spectral features are assigned to d-d transitions originating from the secondary tetrahedral Co(II) ions. FTIR spectra of 3 and 4 exhibit strong but significantly red-shifted bands (ca. 45 cm^{-1} than that of metalloligands 1 and 2) between 1585-1645 cm^{-1} (Fig. S2, ESI). Thermal gravimetric analysis exhibits weight loss of ten and four water molecules between 25-140 °C for complexes 3 and 4, respectively (Fig. S3, ESI) which is well supported from the microanalysis data as well as the crystallographic results. The conductivity measurements assert a 1:1 electrolytic nature for both the trinuclear complexes.[16]

[a.] Department of Chemistry, University of Delhi, Delhi – 110 007 (India). Email: rgupta@chemistry.du.ac.in; Fax: +91-11-27666605; Tel: +91-11-27667624
†Electronic Supplementary Information (ESI) available: [Figures for the absorption, FTIR, NMR spectra; thermal gravimetric analysis; titration studies; catalytic performance; and hot-filtration test; and tables for the crystallographic data collection and structural refinement and detailed bonding parameters]. See DOI: 10.1039/x0xx00000x.

M = Co^{3+} (1)
M = Fe^{3+} (2)

M = Co^{3+} (3)
M = Fe^{3+} (4)

Scheme 1. Synthetic route to trinuclear complexes 3 and 4.

ARTICLE   **Journal Name**

Both heterometallic complexes **3** and **4** have been crystallographically characterized. In each case, the unit cell is comprised of a trimetallic complex anion in addition to one tetraethylammonium cation and a few water molecules.[17] Crystal structures of **3** and **4** show that the secondary Co(II) ions are situated within the molecular clefts created by the appended pyridyl rings (Fig. 1). Both Co(II) ions are additionally coordinated by two chloride atoms thus maintaining a distorted tetrahedral geometry with τ_4 distortion parameter[18] between 0.83-0.86 suggesting a predominantly tetrahedral geometry. For reference, the ideal value of τ_4 for a perfect tetrahedral and square-planar geometry is 1 and 0, respectively.[18] While $N_{pyridine}$ donors form strong bonds (2.04 – 2.06 Å) with the secondary Co(II) ions; Co–Cl bonds are quite longer (2.24 – 2.33 Å). Both structures reveal that the primary metal ion is coordinated to four anionic N_{amide} atoms in the basal plane and two $N_{pyridyl}$ atoms at the axial positions with a compressed octahedral geometry.[19] The central metal is geometrically unaffected by the insertion of secondary Co^{2+} ions; a feature also noted for our earlier trinuclear heterometallic complexes.[19]
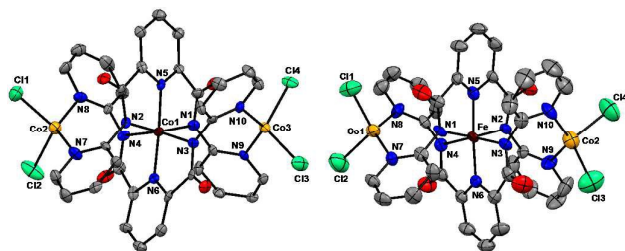

Figure 1. Molecular structures of the anionic parts of trinuclear complexes **3** and **4**. Selected bond distances (Å) and angles (°) for complex **3**: Co(1)-N(1) 1.974(6), Co(1)-N(2) 1.946(6), Co(1)-N(3) 1.967(6), Co(1)-N(4) 1.954(6), Co(1)-N(5) 1.870(6), Co(1)-N(6) 1.861(6), Co(2)-N(7) 2.042(8), Co(2)-N(8) 2.055(6), Co(2)-Cl(1) 2.246(3), Co(2)-Cl(2) 2.248(3), Co(3)-N(9) 2.047(6), Co(3)-N(10) 2.048(6), Co(3)-Cl(3) 2.246(3), Co(3)-Cl(4) 2.253(2), N(5)-Co(1)-N(6) 176.8(3), N(1)- Co(1)-N(2) 161.0(3), N(3)- Co(1)-N(4) 161.5(3), N(7)-Co(2)-N(8) 127.4(3), Cl(1)-Co(2)-Cl(2) 113.4(1), N(9)-Co(3)-N(10) 126.9(2), Cl(3)-Co(3)-Cl(4) 115.56(9). For complex **4**: Fe(1)-N(1) 1.952(5), Fe(1)-N(2) 1.958(5), Fe(1)-N(3) 1.949(6), Fe(1)-N(4) 1.962(5), Fe(1)-N(5) 1.864(4), Fe(1)-N(6) 1.862(4), Co(1)-N(7) 2.039(5), Co(1)-N(8) 2.052(5), Co(1)-Cl(1) 2.240(2), Co(1)-Cl(2) 2.246(3), Co(2)-N(9) 2.060(6), Co(2)-N(10) 2.052(6), Co(2)-Cl(3) 2.233(3), Co(2)-Cl(4) 2.254(3), N(5)- Fe(1)-N(6) 176.4(2), N(1)- Fe(1)-N(2) 161.6(2), N(3)- Fe(1)-N(4) 161.1(2), N(7)-Co(1)-N(8) 126.7(2), Cl(1)-Co(1)-Cl(2) 114.88(9), N(9)-Co(2)-N(10) 126.3(2), Cl(3)-Co(2)-Cl(4) 112.3(1).

Catalytic Nitro Reduction

Considering the presence of exposed secondary Co(II) sites; complexes **3** and **4** offered unique catalytic possibilities for the nitro reduction reactions as the redox-active metals are typically required.[13,14] For reducing agents; hydrazine, particularly hydrazine hydrate, is a suitable choice due to ease in handling and generation of N_2 as the only by-product.[8] Subsequently, both **3** and **4** were tested as the heterogeneous catalysts for the reduction of nitro substrates. Thus, when nitrobenzene was treated with hydrazine in presence of only 1 mol % of **3** or **4** in EtOH; a smooth reaction took place that quantitatively produced aniline.

At this stage, a series of control experiments were performed to identify the best reaction conditions using nitrobenzene as a model substrate and complex **3** as a representative catalyst (Table 1). There was no reaction in the absence of catalyst but presence of hydrazine (entry 1). Use of $CoCl_2$ or $(Et_4N)_2[CoCl_4]$ as the catalyst with assorted reducing agents resulted in negligible conversion (entries 2 – 4). Similarly, catalyst **3** with H_2, NH_4Cl, HCOOH, $NaBH_4$, Ph_3SiH, and $(Me_3Si)_3SiH$ produced insignificant amount of aniline even after 12 h (entries 5 – 10). To our delight, catalyst **3** with hydrazine reduces nitrobenzene to aniline quantitatively within 4 h (entry 11). It was observed that the solvent was essential for the complete conversion as much lower yield was obtained under the solvent-free reaction condition (entry 12). Ethanol was adjudged to be the best solvent (entry 11) as other solvents; CH_3CN, acetone, $CHCl_3$ and THF, provided surprisingly lower yields (entries 13 – 16). Further, moderate conversion was noted when the reduction was performed in higher alcohols such as isopropanol, *n*-butanol, *tert*-butanol (entries 17 – 19). Although both H_2O and MeOH offered quantitative reduction (entries 20 and 21); they were not used subsequently as **3** and **4** have solubility in such solvents and we were interested in heterogeneous catalysis for the practical reasons. The ideal temperature was found to be 60 ˚C as lower temperatures resulted in lower product yield (entry 22). The control experiments further suggested that the reaction requires 4 h and 6 equiv. of hydrazine for completeness (entries 23 and 24). Importantly, complete reduction could also be achieved using only 2 equiv. of hydrazine; however, requires a very small reaction vessel (ca. 1 mL). It is therefore clear that the maintenance of effective pressure created due to in-situ generation of H_2 is essential and a limiting factor. However, all subsequent reactions were performed with 6 equiv. of NH_2NH_2 in a regular Schlenk flask of 5 mL volume for the workable reason.

Expectedly, metalloligand **1** or **2** did not result in any reduction (entry 25). Interestingly, when a 1:2 mixture of metalloligand **1** (or **2**) and $(Et_4N)_2[CoCl_4]$ was used as a catalyst in EtOH; there was practically no reduction of nitrobenzene for the initial 4 h. However, partial reduction was noticed after 6 h while complete reduction to aniline occurred after 24 h (entry 26). This experiment implies *in-situ* formation of {Co^{2+}–Co^{3+}–Co^{2+}} (**3**) or {Co^{2+}–Fe^{3+}–Co^{2+}} (**4**) complexes as the catalyst[20] and further strengthen our point that **3** and **4** act as the *true catalysts* and not as the pre-catalysts and the catalytically active species are not leached out from **3** and **4**.

Reusability experiment, using complex **3**, displayed no loss in activity even after five consecutive catalytic cycles, leading to quantitative reduction with complete selectivity for the 3rd, 4th, and even 5th cycle (Fig. S4, ESI). The hot-filtration test using 1-iodo-4-nitrobenzene as the substrate confirmed that complex **3** functioned as the *true* heterogeneous catalyst (Fig. S5, ESI). This reaction showed quantitative reduction to 1-iodo-4-aminobenzene after 4 h. However, if complex **3** is filtered off after 2 h; the reaction is stopped immediately. Importantly, removal of complex **3** does not lead to any reduction, therefore ruling out the possibility of leaching out of the actual catalyst. More importantly, if complex **3** is

re-added after a gap of 2 h; quantitative reduction was observed after another 2 h. This simple filtration test undoubtedly confirms the heterogeneous nature of the catalysis. Both trinuclear complexes retain their structural integrity and crystallinity during the catalysis. Such a fact is well-supported by the observation of superimposable FTIR spectra (Fig. S6 and S7; ESI) and powder XRD pattern (Fig. S8; ESI) of the recovered complexes to that of pristine samples.

With these optimized reaction conditions, scope of the nitro reduction catalyzed by 3 and 4 was explored (Table 2). The results indicate a generality of catalysis where both 3 and 4 were equally effective. The reduction of nitrobenzene as well as assorted derivatives with diversified substituents was effortless (1a – 1g). We then focused on the possible chemo-selectivity with our heterometallic catalysts and several substrates containing two different functional groups were tested. Importantly, halogen substituted nitroarenes have displayed dehalogenation in earlier catalytic systems.[21] In our case, no dehalogenation was observed both with 3 and 4, independently of the number of halogen atoms and their ring positions, suggesting an excellent control over the chemo-selectivity (1h – 1n). Further, 4-cyano-nitrobenzene was selectively reduced to 4-cyanoaniline (1o), a product of considerable importance in organic synthesis.[22] Along the same direction, 3- as well as 4-nitroethylbenzoates were also exclusively reduced without any effect on the ester group (1p – 1q). Furthermore, bulkier as well as heterocyclic substrates also afforded excellent yield of the corresponding amine (1r – 1w).

Considering high efficiency of the present protocol in reducing nitroarenes to the corresponding anilines; we decided to evaluate the reduction of aliphatic nitro substrates.[23] However, aliphatic nitro substrates (1x and 1y) revealed a significantly lower reactivity toward reduction than that of aromatic analogues as incomplete reduction was noticed with 1 mol% catalyst loading. Satisfyingly, enhancing the catalyst loading to 5 mol% resulted in high conversion for both aliphatic substrates. This reaction places the present complexes at par with some of the most-noted nanoparticle-based catalysts.[13,14,23] It is worth to mention that hydrazine-mediated reduction has not been successful, in compliance with earlier reports,[8,14b] for the substrates containing aldehyde or ketone functional groups since they readily form the corresponding hydrazones. A similar restraint exists for nitroarenes containing olefinic double bonds owing to the fact that diimide, generated as intermediate during the oxidation of hydrazine, can rapidly reduce olefinic double bonds.[14b,24] We encountered both these limitations with catalysts 3 and 4.[25]

Important evidences for the outstanding catalytic activities of 3 and 4 came after the investigation of analogous trinuclear complexes; $\{Cu^{2+}-Co^{3+}-Cu^{2+}\}$ (5) and $\{Cu^{2+}-Fe^{3+}-Cu^{2+}\}$ (6),[19d] having structures nearly identical to that of 3 and 4 (Scheme 2). Interestingly, both 5 and 6 were found to be somewhat catalytically active for the hydrazine-based reduction of nitrobenzene. However, in both cases, in addition to unreacted nitrobenzene (45-60%); aniline (30–35%), azo- and azooxy- (10-20%) products were

obtained. Such an observation is noteworthy and suggests that while complexes 5 and 6 participate in the reduction of nitrobenzene; they are only active to some extent but not efficient and selective as that of 3 and 4. We then used complex 7 (Scheme 2) for the catalysis which mimics the partial structure of heterometallic complexes 3 and 4 by showcasing a Co(II) ion coordinated by two $N_{phenanthroline}$ donors (2.046 Å) and two chloride atoms (2.2030 Å).[26] Interestingly, complex 7 caused only 8% reduction of nitrobenzene using hydrazine under the otherwise identical reaction conditions. To rule out the possible steric hindrance caused due to the presence of methyl groups at 2 and 9 positions of phenanthroline ligand; complex 7 was used for the un-optimized ring-opening reactions of a few sterically cumbersome epoxides. Notably, complex 7 was able to provide the respective products in reasonable yield therefore ruling out the substrate accessibility as an issue (see Table S3, ESI). Collectively, these experiments conclusively prove the uniqueness of heterometallic complexes 3 and 4 in the reduction of nitro group.
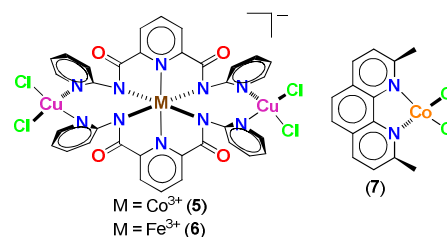
Scheme 2. Chemical drawings of trinuclear complexes 5 and 6 and a mononuclear complex 7.

Mechanistic Aspects

To shed light on the probable mechanism; absorption spectra were measured.[27] Thus, when incremental aliquots of hydrazine were added to a DMF solution of complex 3 or 4; disappearance of the spectral bands centered at 608 and 675 nm occurred (Fig. 2 and 3). Notably, these spectral titrations unambiguously confirmed the stoichiometry of 1:0.5 between the trinuclear complexes $\{Co^{2+}-Co^{3+}-Co^{2+}\}$ (3) and $\{Co^{2+}-Fe^{3+}-Co^{2+}\}$ (4) to that of hydrazine (see insets in Fig. 2 and 3). Importantly, in case of 3; the resultant spectrum is almost identical to that of metalloligand 1 suggesting no or negligible contribution from the secondary cobalt ions (see Inset of Fig. 4).[28,29]
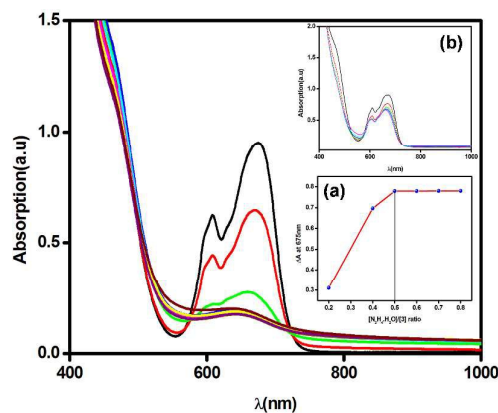
Figure 2. Absorption spectral titration of complex **3** with hydrazine in DMF and their stoichiometry after monitoring the spectral change at 675 nm (inset a). The inset b shows a similar titration of complex **3** with two equiv. of phenylhydrazine. See text for details.
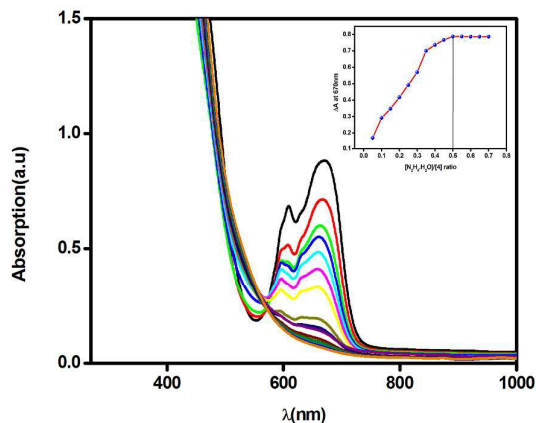

Figure 3. Spectral titration of complex **4** with hydrazine in DMF and their stoichiometry after monitoring the spectral change at 670 nm (inset).

The spectral bands centered at 608 and 675 nm are assigned to d-d transitions originating from the secondary tetrahedral Co(II) ions which disappeared during the reaction with hydrazine. We, therefore, suggest that the disappearance of such spectral bands is associated with the reduction of secondary Co(II) ions to transient Co(I) ions. The stoichiometry further asserts that only 0.5 equivalent of hydrazine is required for supplying two electrons per trinuclear complex. More importantly, the original spectral features are quantitatively regenerated after oxidation either with 2 equiv. of $FcPF_6$ or 2 equiv. of bromine or excess O_2 (Fig. 4). Such a proposal advocates a redox reaction between complex **3** or **4** to that of hydrazine where hydrazine is first oxidized to diimide then finally to dinitrogen. In the process, liberated electrons and protons reduce the nitro group to amine. Interestingly, addition of up to two equivalents of phenylhydrazine caused only 20% reduction of the Co(II) spectral features (*see* Inset b; Fig. 2); therefore, suggesting incomplete reduction due to the weaker reducing ability of phenylhydrazine. In fact, use of phenylhydrazine as the reducing agent only caused less than 5% reduction of nitrobenzene using complex **3** as a catalyst (data not shown) thus justifying the spectral titration results.
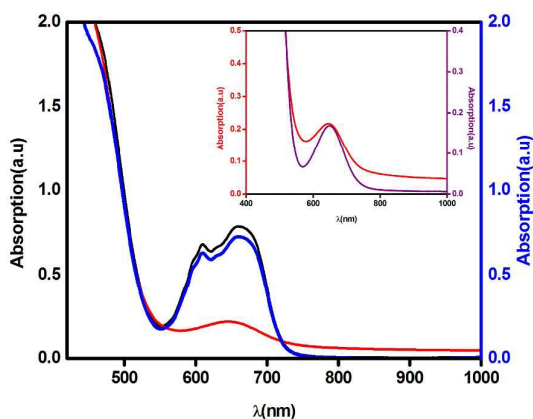

Figure 4. Absorption spectrum of complex **3** (black trace); after the addition of 0.5 equivalent of hydrazine (red trace); after the addition of 1 equivalent of bromine (blue trace). Inset shows the spectral comparison of pristine complex **1** and the one generated after the reaction between complex **3** and 0.5 equivalent of hydrazine.

We then attempted to ascertain whether a similar reaction with hydrazine takes place either with metalloligands **1** and **2**; complexes **5** and **6** or even complex **7**. Notably, there was no reaction of metalloligands **1** and **2** even with excess hydrazine (Fig. S9 and S10, ESI); in line with the negative results for the reduction of nitrobenzene (*cf.* entry 25; Table 1). Importantly, complex **5** displayed a similar observation as noted for **3** and **4**; where spectral features centered on 680 and 875 nm were quenched after the addition of 0.5 equiv. of hydrazine and restored after oxidation with Br_2 (Fig. 5 and 6).[30] More importantly, complex **7** behaved differently. While addition of 0.25 equiv. of hydrazine did result in the disappearance of spectral features centered at 575 and 650 nm; oxidation with Br_2 caused the generation of a slightly different Co(II) complex with λ_{max} at 670 nm with a weak shoulder at 590 nm (Fig. S11, ESI). These experiments suggest that while complexes **5** and **6** behave similarly to that of **3** and **4**; complex **7** stands out and does not support a reversible oxidation-reduction reaction with hydrazine. We, therefore, assert that the lack of reversibility is the key aspect behind the poor performance of complex **7** despite offering a close structural feature as in **3** and **4**.
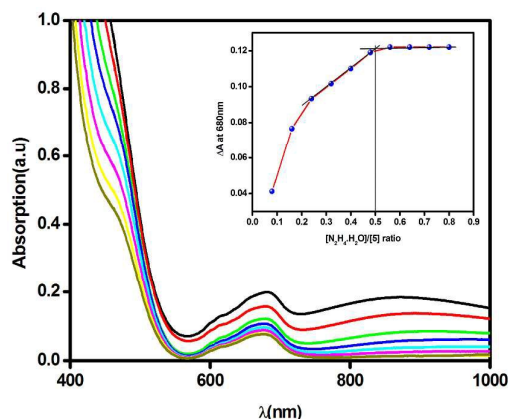

Figure 5. Absorption spectral titration of complex **5** with hydrazine in DMF. Inset shows the stoichiometry between complex **5** and hydrazine after monitoring the spectral change at 680 nm.

Mechanistically, nitrobenzene reduction proceeds through a few intermediates such as nitrosobenzene and *N*-phenylhydroxylamine (Scheme 3).[31] Subsequently, nitrosobenzene and *N*-phenylhydroxylamine intermediates could either directly proceed to aniline (pathway **A**) or could combine to produce azoxybenzene, azobenzene, and 1,2-diphenylhydrazine intermediates (pathway **B**). The number(s) and quantity of such intermediates depend upon the catalyst, substrate, solvent, temperature, and reaction time.[23] To elucidate the reaction pathways out of **A** or **B**; absorption spectra were measured during the reaction between nitrobenzene and hydrazine (Fig. S12, ESI). The absorption spectrum of the reaction mixture recorded after 1 h only displayed bands at 286 and 315 nm assigned to aniline and

nitrosobenzene, respectively.[23] Notably, after 4h of the reaction; band for nitrosobenzene disappeared completely leaving behind the only band of aniline. Such an exercise validates that the reaction proceeds through the intermediacy of nitrosobenzene and *N*-phenylhydroxylamine (pathway **A**) and not via azoxybenzene, azobenzene, and 1,2-diphenylhydrazine (pathway **B**). Further evidences came from the separate reactions of the proposed intermediates with hydrazine in presence of complexes **3** or **4**. Importantly, complexes **3** and **4** individually reduced nitrosobenzene as well as *N*-phenylhydroxylamine to aniline quantitatively in presence of hydrazine therefore advocating pathway **A**. More importantly, if azoxybenzene or azobenzene were employed as the substrates; the reaction exclusively stops at 1,2-diphenylhydrazine as the product but not leading to aniline even in presence of excess hydrazine or prolonged reaction time. All these experiments establish the operation of pathway **A** and ruling out the pathway **B**. On the other hand, related trinuclear complexes **5** and **6**[19d] do produce azoxybenzene and azobenzene intermediates thus supporting the pathway **B**; however, are not efficient catalysts. It is therefore clear that a Co(II) ion is a far better choice than that of a Cu(II) ion for the nitro reduction and may help in designing better catalytic systems in future.
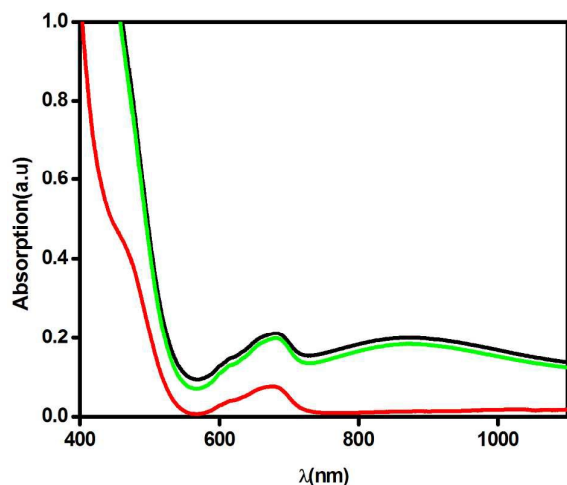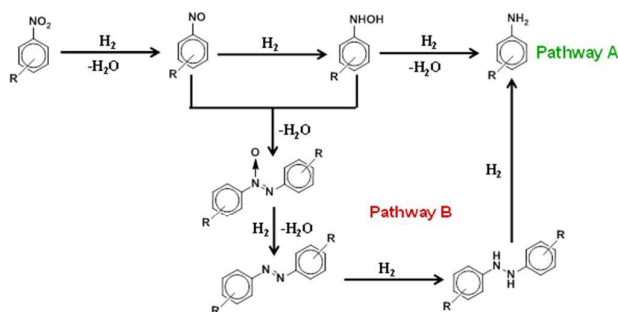

Figure 6. UV/Vis spectrum of complex **5** (black trace); complex **5** after the addition of 0.5 equivalent of hydrazine (red trace); after the addition of 1 equivalent of bromine (green trace).

Scheme 3. Proposed mechanism for the hydrazine-mediated reduction of nitroarenes.

Conclusions

In conclusion, we have displayed reduction of assorted nitro compounds utilizing $\{Co^{2+}-Co^{3+}-Co^{2+}\}$ and $\{Co^{2+}-Fe^{3+}-Co^{2+}\}$ complexes. Both complexes functioned as the reusable heterogeneous catalysts with excellent product selectivity. The mechanistic investigations suggested the involvement of Co(II)-Co(I) cycle in the catalysis. Our results illustrate the uniqueness and importance of discrete complexes in understanding a challenging organic reaction and the future work is directed to explore similar molecular complexes in other challenging reactions.

Experimental

General

The reagents and chemicals were obtained from the commercial sources and were used as received. The solvents were dried and/or purified as per the standard literature.[32] Complexes $Et_4N[CoL_2]$ (**1**) and $Et_4N[FeL_2]$ (**2**) (where $H_2L = N^2,N^6$-di(pyridin-2-yl)pyridine-2,6-dicarboxamide) were synthesized as per our earlier reports.[19]

Syntheses

$Et_4N[(\mathbf{1})(CoCl_2)_2]$ (**3**). To a solution of **1** (0.100 g, 0.12 mmol) in 15 ml DMF, anhydrous $CoCl_2$ (0.039 g, 0.30 mmol) was added as the solid under the dinitrogen atmosphere. The resulting reaction mixture was stirred for 1 h at 25 °C. The solution was filtered and the volatiles were removed under the reduced pressure to afford a green solid. The crystallization was achieved by the vapour diffusion of diethyl ether to a DMF solution of the crude product at 25 °C which afforded highly crystalline product within 1 d. Yield: 0.014 g (92 %). Anal. Calcd. for $C_{42}H_{42}N_{11}O_4CoCo_2Cl_4\cdot10H_2O$ (1263.62): C, 39.92; H, 4.95; N, 12.19. Found: C, 39.61; H, 4.65; N, 12.46. FTIR spectrum (Zn-Se ATR, selected peaks): 3447, 1642, 1595 cm^{-1}. Conductivity (DMF, ~1mM, 298K): $\Lambda_M = 50$ $\Omega^{-1}cm^2mol^{-1}$. Absorption spectrum [λ_{max}, nm, DMF (ϵ, M^{-1} cm^{-1})]: 675 (990), 608 (640).

$Et_4N[(\mathbf{2})(CoCl_2)_2]$ (**4**). This complex was synthesized in a similar manner using an identical scale as discussed for **3**; however using **2**. The product was isolated as green solid which was further recrystallized by the vapour diffusion of diethyl ether to a DMF solution of the crude product. Yield: 0.012 g (86 %). Anal. Calcd. for $C_{42}H_{42}Cl_4Co_2FeN_{11}O_4\cdot4H_2O$ (1152.4): C 43.77, H 4.37, N 13.37; found C 43.58, H 4.49, N 13.71. FTIR spectrum (Zn-Se ATR, selected peaks): 3472, 1634, 1599 cm^{-1}. Conductivity (DMF, ~1Mm, 298 K): $\Lambda_M = 45$ $\Omega^{-1}cm^2mol^{-1}$. Absorption spectrum [λ_{max}, nm, DMF (ϵ, M^{-1} cm^{-1})]: 675 (880), 608 (560).

General Procedure for the Reduction of Nitro-Substrate

To a Schlenk reaction flask, nitro substrate (1.0 mmol) was taken in EtOH (2 ml) and the catalyst (1 mol%) was added. The content was stirred for 5 m followed by the addition of hydrazine monohydrate (6.0 mmol) under inert conditions. The reaction mixture was stirred at 60 °C for 2-12 h while the progress of the reaction was monitored by the gas chromatograph (GC). After completion, catalyst was

filtered off, washed with EtOH, and dried in vacuum. The filtrate was passed through a plug of 100–200 mesh silica and concentrated to afford the organic product. Products were identified and/or characterized by the GC, GC-MS, and ^{1}H NMR spectra wherever required.

Characterization Data for a Few Representative Products

The ^{1}H and ^{13}C NMR spectral data for a few representative products[33-35] are provided below whereas the respective figures are included as the Fig. S15 – S24 (ESI).

4-Aminotoluene (**1b**): Isolated Yield: 94%. ^{1}H NMR spectrum (400MHz, CDCl$_3$): δ= 7.01-6.99 (d, 2H), 6.64-6.62 (d, 2H), 3.49 (s, 2H) 2.28 (s, 3H). ^{13}C NMR spectrum (100MHz, CDCl$_3$): δ= 143.97, 129.83, 127.87, 115.40, 20.59.

4-Chloroaniline (**1i**): Isolated Yield: 93%. ^{1}H NMR spectrum (400MHz, CDCl$_3$): δ= 6.97-6.95 (d, 2H), 6.51-6.49 (d, 2H), 5.16 (s, 2H). ^{13}C NMR spectrum (100MHz, CDCl$_3$): δ= 148.17, 129.01, 119.24, 115.70.

4-Aminobenzonitrile (**1o**): Isolated Yield: 96%. ^{1}H NMR spectrum (400MHz, CDCl$_3$): δ= 7.21-7.23 (d, 2H), 6.52-6.54 (d, 2H), 3.55(s, 2H). ^{13}C NMR spectrum (100MHz, CDCl$_3$): δ= 145.59, 132.10, 116.86, 110.21.

Ethyl-4-aminobenzoate (**1q**): Isolated Yield: 95%. ^{1}H NMR spectrum (400MHz, CDCl$_3$): δ= 7.58-7.60 (d, 2H), 6.50-6.53 (d, 2H), 5.89 (s, 2H), 4.11-4.46 (q, 2H), 1.18-1.22 (t, 3H). ^{13}C NMR spectrum (100MHz, CDCl$_3$): δ= 166.42, 153.92, 131.83, 116.57, 113.15, 60.00, 14.84.

1-Napthylamine (**1r**): Isolated Yield: 95%. ^{1}H NMR spectrum (400MHz, CDCl$_3$): δ= 7.82-7.79 (m, 2H), 7.48-7.43 (m, 2H), 7.33-7.24 (m, 2H), 6.79-6.77 (m, 1H), 4.08(s, 2H). ^{13}C NMR spectrum (100MHz, CDCl$_3$): δ= 142.16, 134.49, 128.65, 126.43, 125.95, 124.96, 123.75, 120.89, 119.68, 109.79.

Physical Methods

The FTIR spectra were recorded with Perkin-Elmer Spectrum-Two spectrometer having Zn-Se ATR. The NMR spectroscopic measurements were carried out with a Jeol 400 MHz spectrometer using TMS as the internal standard. The solution absorption spectra were recorded with Perkin-Elmer Lambda 25 spectrophotometer. The elemental analysis data were obtained with an Elementar Analysen Systeme GmbH Vario EL-III instrument. GC and GC–MS studies were performed with either with a Perkin Elmer Clarus 580 or a Shimadzu instrument (QP 2010) with an RTX-5SIL-MS column. Thermal gravimetric analysis (TGA) was performed with DTG 60 Shimadzu at 5 °C min^{-1} heating rate under the dinitrogen atmosphere.

Crystallography

Single crystals suitable for the X-ray diffraction studies were grown by vapour diffusion of diethyl ether into a DMF solution of complexes **3** and **4**. The intensity data were collected at 298 K with an Oxford XCalibur CCD diffractometer equipped with a graphite

monochromatic Mo-*K*α radiation (*λ* = 0.71073 Å).[36] An empirical absorption correction was applied using spherical harmonics implemented in the SCALE3 ABSPACK scaling algorithm.[36] The structures were solved by the direct methods using SIR-97[37] and refined by the full-matrix least-squares refinement techniques on F^2 using the program SHELXL-97[38] in the WinGX crystallographic module.[39] All hydrogen atoms were fixed at the calculated positions with isotropic thermal parameters whereas all non-hydrogen atoms were refined anisotropically. Attempts to refine peaks of residual electron density as guest atoms in complex **3** were unsuccessful; although atoms of water molecules were observed but could not be modelled satisfactorily during the structure refinement. Therefore data were corrected for the disordered electron density by using the SQUEEZE procedure implemented in PLATON.[40] A total solvent-accessible void volume of 446.0 x 10^{-3} Å^3 with a total electron count of 103 (consistent with ca. ten water molecules per formula) was found in the unit cell. The presence of 10 lattice water molecules was further confirmed by the thermal studies as well as microanalytical data. Details of the crystallographic data collection and structural solution parameters are provided in Table S1 whereas the detailed bond length and bond angles around the central/peripheral metal atoms are collected in Table S2.

Acknowledgements

Notes and references

1 N. Ono, *The Nitro Group in Organic Synthesis*, Wiley-VCH, New York, 2001.
2 a) S. Nishimura, *Handbook of Heterogeneous Catalytic Hydrogenation for Organic Synthesis*, Wiley-Interscience, New York, 2001; b) H. Arnold, F. Dobert, and J. Gaube, *Handbook of Heterogeneous Catalysis*, Wiley-Interscience, New York, 2008, pp. 3266 – 3284.
3 a) H. U. Blaser, H. Steiner, and M. Studer, *ChemCatChem*, 2009, **1**, 210; b) H. U. Blaser, U. Siegrist, H. Steiner, and M. Studer, In *Fine Chemicals through Heterogeneous Catalysis*, ed. R. A. Sheldon, and H. van Bekkum, Wiley-VCH, Weinheim, 2001, pp. 389.
4 a) K. Junge, B. Wendt, N. Shaikh, and M. Beller, *Chem. Commun.* 2010, **46**, 1769; b) L. Pehlivan, E. Metay, S. Laval, W. Dayoub, P. Demonchaux, G. Mignani, and M. Lemaire, *Tetrahedron Lett.* 2010, **51**, 1939.
5 J. W. Bae, Y. J. Cho, S. H. Lee, C. O. M. Yoon, and C. M. Yoon, *Chem. Commun.* 2000, 1857.
6 H. Berthold, T. Schotten, and H. Honig, *Synthesis*, 2002, 1067.
7 a) G. Wienhçfer, I. Sorribes, A. Boddien, F. Westerhaus, K. Junge, H. Junge, R. Llusar, and M. Beller, *J. Am. Chem. Soc.* 2011, **133**, 12875; b) I. Sorribes, G. Wienhofer, C. Vicent, K. Junge, R. Llusar, and M. Beller, *Angew. Chem. Int. Ed.* 2012, **51**, 7794.
8 a) A. Vass, J. Dudas, J. Toth, and R. S. Varma, *Tetrahedron Lett.* 2001, **42**, 5347; b) M. Kumarraja, and K. Pitchumani, *Appl. Catal. A* 2004, **265**, 135; c) Q. Shi, R. Lu, K. Jin, Z. Zhang, and D. Zhao, *Green Chem.* 2006, **8**, 868; d) S. Kim, E. Kim, and
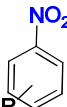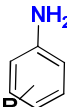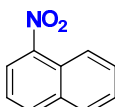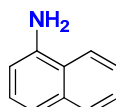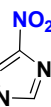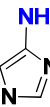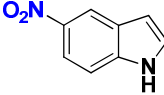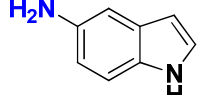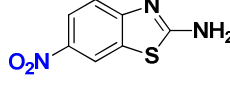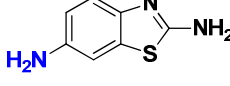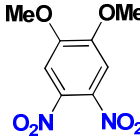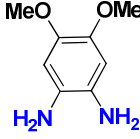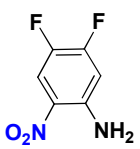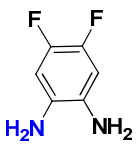
B. M. Kim, *Chem. Asian J.* 2011, **6**, 1921; e) U. Sharma, P. K. Verma, N. Kumar, V. Kumar, M. Bala, and B. Singh, *Chem. Eur. J.* 2011, **17**, 5903; f) R. V. Jagadeesh, F. A. Wienhöfer, G. Westerhaus, A.-E. Surkus, M.-M. Pohl, H. Junge, K. Junge, and M. Beller, *Chem. Commun.* 2011, **47**, 10972; g) Z. Zhao, H. Yang, Y. Li, and X. Guo, *Green. Chem.* 2014, **16**, 1274.

9   X. Lin, M. Wu, D. Wu, S. Kuga, T. Endoe, and Y. Huang, *Green Chem.* 2011, **13**, 283.

10 A. M. Tafesh and J. Weiguny, *Chem. Rev.* 1996, **96**, 2035.

11 a) A. Corma and P. Serna, *Science*, 2006, **313**, 332; b) L. He, L.-C. Wang, H. Sun, J. Ni, Y. Cao, H.-Y. He, and K.-N. Fan, *Angew. Chem., Int. Ed.* 2009, **48**, 9538; c) M. Li, L. Hu, X. Cao, H. Hong, J. Lu, and H. Gu, *Chem. Eur. J.* 2011, **17**, 2763; d) H. Wu, L. Zhuo, Q. He, X. Liao, and B. Shi, *Appl. Catal., A* 2009, **366**, 44; e) A. J. Amali, and R. K. Rana, *Green Chem.* 2009, **11**, 1781l; f) J. Li, X. Shi, Y. Bi, J. Wei, and Z. Chen, *ACS Catal.* 2011, **1**, 657.
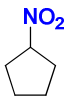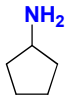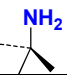
12 a) *Nanoparticles and Catalysis*; D. Astrus, Ed.; Wiley-VCH: Weinheim, Germany, 2008; b) E. Boymans, S. Boland, P. T. Witte, C. Muller, and D. Vogt, *ChemCatChem* 2013, **5**, 431; c) H-U. Blaser, H. Steiner, and M. Studer, *ChemCatChem* 2009, **1**, 210.

13 F. A. Westerhaus, R. V. Jagadeesh, G. Weinhofer, M.-M. Pohl, J. Radnik, A.-E. Surkus, J. Rabeah, K. Junge, H. Junge, M. Nielsen, A. Bruckner, and M. Beller, *Nat. Chem.* 2013, **5**, 537.

14 a) D. Cantillo, M. Baghbanzadeh, and C. O. Kappe, *Angew. Chem. Int. Ed.* 2012, **51**, 10190; b) D. Cantillo, M. M. Moghaddam, and C. O. Kappe, *J. Org. Chem.* 2013, **78**, 4530; c) X. Gu, Z. Sun, S. Wu, W. Qi, H. Wang, X. Xu, and D. Su, *Chem. Commun.* 2013, **49**, 10088.

15 G. Kumar and R. Gupta, *Chem. Soc. Rev.* 2013, **42**, 9403.

16 W. J. Geary, *Coord. Chem. Rev.* 1971, **7**, 81.

17 For complex **3**; ten disordered water molecules were squeezed using the SQUEEZ routine command of PLATON.

18 L. Yang, D. R. Powell, and R. P. Houser, *Dalton Trans.* 2007, 955.

19 a) A. Mishra, A. Ali, S. Upreti, and R. Gupta, *Inorg. Chem.* 2008, **47**, 154; b) A. Mishra, A. Ali, S. Upreti, M. S. Whittingham, and R. Gupta, *Inorg. Chem.* 2009, **48**, 5234; c) A. P. Singh and R. Gupta, *Eur. J. Inorg. Chem.* 2010, 4546; d) S. Srivastava, A. Ali, A. Tyagi, and R. Gupta, *Eur. J. Inorg. Chem.* 2014, 2113; e) S. Srivastava, M. S. Dagur, and R. Gupta, *Eur. J. Inorg. Chem.* 2014, 4966.

20 Absorption spectrum of the product from the reaction mixture exhibits Co(II) specific bands at 608 and 675 nm while suggesting the formation of **3** and **4** in nearly 90% yield.

21 R. J. Rahaim and R. E. Maleczka, *Org. Lett.* 2005, **7**, 5087.

22 C. M. Marson, *Chem. Soc. Rev.* 2011, **40**, 5514.

23 R. K. Rai, A. Mahata, S. Mukhopadhyay, S. Gupta, P.-Z. Li, K. T. Nguyen, Y. Zhao, B. Pathak, and S. K. Singh, *Inorg. Chem.* 2014, **53**, 2904.

24 M. Lamani, G. S. Ravikumar, and K. R. Prabhu, *Adv. Synth. Catal.* 2012, **354**, 1437.

25 Benzaldehyde forms the respective hydrazone with hydrazine in presence of **3** or **4**, thus suggesting a general nature of such a reaction. Although alternative reducing agents such as silanes or siloxanes could be used for such substrates and we do have plans to explore such avenues.

26 N. A. Torbati, A. R. Rezvani, N. Safari, V. Amani, H. R. Khavasi, *Acta Cryst*. 2010, **E66**, m1236.

27 Both **3** and **4** are EPR silent and remain EPR silent after the addition of hydrazine; however, ^{1}H NMR spectra do exhibit noticeable changes after the reaction with hydrazine; see Fig. S13 and S14 (ESI).

28 In case of **4**; we were not able to correlate the spectral features to that of metalloligand **2** due to the occurrence of λ_{max} at UV region and interference from hydrazine and product.

29 We do not have evidence if the resultant Co(I) ions remain bound to the metalloligand; although, we tend to believe that the trimetallic core remain intact during the catalysis as evidenced by the restoration of complexes **3** and **4** after oxidation and catalytic recycling experiments (*cf.* Fig. S4 and S5, ESI).

30 Complex **6** could not be tested due to the limited solubility.

31 R. M. Dyson, M. Hazenkamp, K. Kaufmann, M. Maeder, M. Studer, and A. Zilian, *J. Chemometrics*, 2000, **14**, 737.

32 D. D. Perrin, W. L. F. Armarego, and D. R. Perrin, *Purification of Laboratory Chemicals*, Pergamon Press, Oxford, UK, 1980.

33 D. Cantillo, M. M. Moghaddam, and C. O. Kappe, *J. Org. Chem.* 2013, **78**, 4530.

34 Z. Zhao, H. Yang, Y. Li, and X. Guo, *Green Chem.* 2014, **16**, 1274.

35 Y. S. Feng, J. J. Ma, Y. M. Kang, and H. J. Xu, *Tetrahedron*, 2014, **70**, 6100.

36 *CrysAlisPro*, v. 1.171.33.49b, Oxford Diffraction Ltd., Abingdon, 2009.

37 A. Altomare, G. Cascarano, C. Giacovazzo, and A. Guagliardi, *J. Appl. Crystallogr.* 1993, **26**, 343.

38 G. M. Sheldrick, *Acta Crystallogr., Sect. A* 2008, **64**, 112.

39 L. J. Farrugia, WinGX, v. 1.70, An Integrated System of Windows Programs for the Solution, Refinement and Analysis of Single- Crystal X-ray Diffraction Data, Department of Chemistry, University of Glasgow, 2003.

40 A. L. Spek, PLATON, A Multipurpose Crystallographic Tool, Utrecht University, The Netherlands, 2002.

Table 1. Control and optimization experiments using $PhNO_2$ as the model substrate with assorted catalysts and/or reaction conditions.[a]

S. No.	Catalyst	Reducing Agent	Solvent, temp. or condition	Yield (%)[k]
1	---	NH_2NH_2	EtOH	0
2[b]	$CoCl_2$ or $(Et_4N)_2CoCl_4$	H_2[c]	EtOH	0
3[b]	$CoCl_2$ or $(Et_4N)_2CoCl_4$	$NaBH_4$	EtOH	5
4[b]	$CoCl_2$ or $(Et_4N)_2CoCl_4$	NH_2NH_2	EtOH	2
5[d]	**3**	H_2[c]	EtOH	2
6[d]	**3**	NH_4Cl	EtOH	0
7[d]	**3**	HCO_2H	EtOH	0
8[d]	**3**	$NaBH_4$	EtOH	6
9[d]	**3**	Ph_3SiH	EtOH	0
10[d]	**3**	$(Me_3Si)_3SiH$	EtOH	0
11[e]	**3**	NH_2NH_2	EtOH	100
12	**3**	NH_2NH_2	Solvent-free	15,[f] 25[g]
13	**3**	NH_2NH_2	MeCN	3
14	**3**	NH_2NH_2	Acetone	2
15	**3**	NH_2NH_2	$CHCl_3$	1
16	**3**	NH_2NH_2	THF	10
17	**3**	NH_2NH_2	Isopropanol	15
18	**3**	NH_2NH_2	^nBuOH	30
19	**3**	NH_2NH_2	^tBuOH	55
20	**3**	NH_2NH_2	MeOH	100
21	**3**	NH_2NH_2	H_2O	100
22	**3**	NH_2NH_2	30, 40, 60, 80 °C	45, 70, 100, 100
23	**3**	NH_2NH_2	1, 2, 3, 4, 5 h	40, 50, 70, 100, 100
24	**3**	2, 4, 6 equiv. NH_2NH_2	EtOH	20, 60, 100
25	**1** or **2**	NH_2NH_2	EtOH	0
26	**1** or **2** + $(Et_4N)_2CoCl_4$	NH_2NH_2	EtOH	0,[h] 20,[i] 100[j]

[a]Conditions: catalyst–1 mol%; temperature: 60 °C; reaction time: 6 h; yield was calculated using the gas chromatograph. [b]5 mol% catalyst. [c]1 atmosphere. [d] Reaction time: 12 h. [e] Reaction time: 4 h. [f] Temperature: 30 °C. [g] Temperature: 60 °C. [h] Reaction time: 4 h. [i] Reaction time: 6 h. [j]Reaction time: 24 h. [k]The yields are the average of 2/3 independents sets.

Table 2. Reduction of assorted nitro substrates using hydrazine in presence of complex **3** or **4** as the catalyst.[a]

Entry	Substrate	Catalyst (mol%)	Product	Yield (%)[b] with **3**	Yield (%)[b] with **4**
	(nitrobenzene with R)		(aniline with R)		
1a	R = H	1	R= H	>99	>99
1b	R = 4-OMe	1	R = 4-OMe	>99	>99
1c	R = 3-NH$_2$	1	R = 3-NH$_2$	>99	>99
1d	R = 4-NH$_2$	1	R = 4-NH$_2$	>99	>99
1e	R = 2,3-NH$_2$	1	R = 2,3-NH$_2$	>99	>99
1f	R = 3-NO$_2$	1	R = 3-NH$_2$	>99	>99
1g	R = 4-NO$_2$	1	R = 4-NH$_2$	>99	>99
1h	R = 3-Cl	1	R = 3-Cl	94	93
1i	R = 4-Cl	1	R = 4-Cl	92	95
1j	R = 2-Br	1	R = 2-Br	>99	95
1k	R = 4-Br	1	R = 4-Br	96	94
1l	R = 2,5-Br	1	R = 2,5-Br	>99	>99
1m	R = 3-I	1	R = 3-I	99	99
1n	R = 4-I	1	R = 4-I	99	99
1o	R = 4-CN	1	R = 4-CN	98	95
1p	R = 3-COOEt	1	R = 3-COOEt	>99	>99
1q	R = 4-COOEt	1	R = 4-COOEt	>99	>99
1r	(1-nitronaphthalene)	1	(1-aminonaphthalene)	>99	99
1s	(nitroimidazole)	1	(aminoimidazole)	99	99
1t	(5-nitroindole)	1	(5-aminoindole)	94	95
1u	(6-nitro-2-aminobenzothiazole)	1	(6-amino-2-aminobenzothiazole)	99	99
1v	(dimethoxy dinitrobenzene)	1	(dimethoxy diaminobenzene)	99	99
1w	(difluoro nitroaniline)	1	(difluoro diaminobenzene)	99	99
1x	(nitrocyclopentane)	5	(aminocyclopentane)	65	67
1y	(nitro compound)	5	(amino compound)	75	80

[a]Conditions: temperature: 60 °C; reaction time: 6 h; yield was calculated using the gas chromatograph. [b]The yields are the average of 2/3 independents sets.

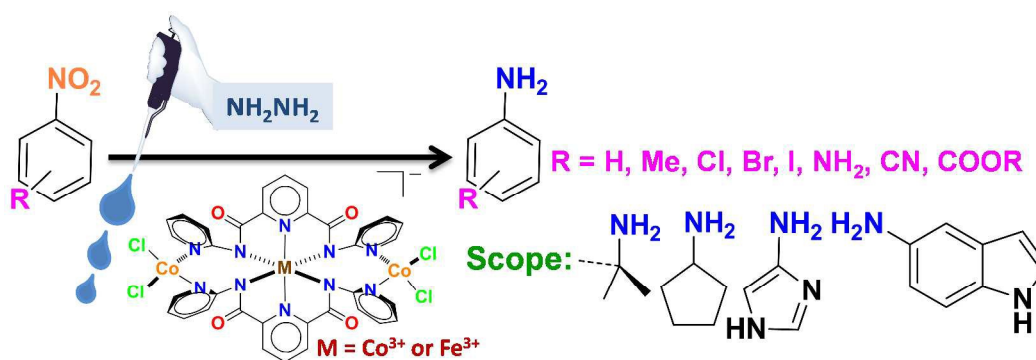# Graphical Abstract

Trinuclear {Co^{2+}-M^{3+}- Co^{2+}} Complexes Catalyze Reduction of Nitro Compounds

Sumit Srivastava, Manvender S Dagur, Afsar Ali, and Rajeev Gupta*

Department of Chemistry, University of Delhi, Delhi – 110 007 (India)

Artwork:

Synopsis: Trinuclear {Co^{2+}–Co^{3+}–Co^{2+}} and {Co^{2+}–Fe^{3+}–Co^{2+}} complexes function as the reusable heterogeneous catalysts for the selective reduction of assorted nitro compounds to their corresponding amines. The mechanistic investigations suggest the involvement of Co(II)-Co(I) cycle in the catalysis.